(-)-Epigallocatechin-3-gallate mitigates cyclophosphamide-induced intestinal injury by modulating the tight junctions, inflammation and dysbiosis in mice

Journal:	*Food & Function*
Manuscript ID	FO-ART-06-2021-001848.R1
Article Type:	Paper
Date Submitted by the Author:	18-Sep-2021
Complete List of Authors:	Wei, Ran; Zhejiang Agriculture and Forestry University, Tea Science Liu, Xingquan; Zhejiang Agriculture and Forestry University, Food Science Wang, Yuefei; Zhejiang University, Dong, Junjie; Zhejiang Camel Transworld Organic Food Co Wu, Fenghua; Zhejiang Agriculture and Forestry University, Food Science Mackenzie, Gerardo; University of California Davis, Nutrition Su, Zhucheng; Zhejiang Agriculture and Forestry University, Tea Science

SCHOLARONE™
Manuscripts

(-)-Epigallocatechin-3-gallate mitigates cyclophosphamide-induced intestinal injury by modulating the tight junctions, inflammation and dysbiosis in mice

Ran Wei[1], Xingquan Liu[2], Yuefei Wang[3], Junjie Dong[4], Fenghua Wu[2], Gerardo G. Mackenzie[5,*], Zhucheng Su[1,*]

[1]Department of Tea Science, Zhejiang Agriculture and Forestry University, Hangzhou, 311300, China.
[2]Department of Food Science, Zhejiang Agriculture and Forestry University, Hangzhou, 311300, China.
[3]Institute of Tea Science, Zhejiang University, Hangzhou, 310058, China.
[4]Zhejiang Camel Transworld Organic Food Co., Ltd, Hangzhou, 310041, China.
[5]Department of Nutrition, University of California, Davis, California, 95616, USA.

[*]Corresponding authors:

Dr. Gerardo G. Mackenzie, Ph.D.
Department of Nutrition, University of California, Davis
One Shields Ave. Davis, CA, 95616
Phone: (530) 752-2140; Fax: (530) 752-8966;
E-mail: ggmackenzie@ucdavis.edu

Dr. Zhucheng Su, Ph.D.
Department of Tea Science, Zhejiang Agriculture and Forestry University
Hangzhou, Zhejiang, 311300, China
Phone:(0571) 63743302
E-mail: zhuchengsu@zafu.edu.cn

Running title: EGCG alleviates cyclophosphamide-induced intestinal damage

Abstract

Cyclophosphamide (CTX) is an antitumor drug commonly used to treat various cancer types. Unfortunately, its toxic side effects, including gastrointestinal (GI) toxicity, affect treatment compliance and patients' prognosis. Thus, there is a critical need of evaluating strategies that may improve the associated GI toxicity induced by CTX. In this work, we evaluated the capacity of Epigallocatechin-3-gallate (EGCG), a major constituent of green tea, to improve the recovery of gut injury induced by CTX in mice. Treatment with CTX for 5 days severely damaged the intestine structure, increased immune-related cytokines (TNFα, IL-10 and IL-21), reduced the expression levels of tight junctions proteins (ZO-1, Occludin, Claudin-1), induced reactive oxygen species, altered the composition of gut microbiota, and reduced short chain fatty acids levels. EGCG treatment, starting one day after the last CTX dose, significantly improved the intestine structure, ameliorated gut permeability, and restored ZO-1, Occludin and Claudin-1 levels. Moreover, EGCG reduced TNFα, IL-10 and IL-21 levels, and decreased oxidative stress via regulating the activity of the antioxidant enzymes catalase, superoxide dismutase and glutathione peroxidase. Finally, EGCG treatment restored the composition of gut microbiota and the levels of the short chain fatty acids. In conclusion, these findings indicate that EGCG may function as an effective bioactive to minimize CTX-induced GI tract toxicity.

Keywords: EGCG, gastrointestinal tract, cyclophosphamide, intestinal inflammation, tight junctions, dysbiosis

1. Introduction

The alkylating agent cyclophosphamide (CTX) is an anticancer agent with more than 40 years of clinical use[1]. To date, CTX remains a mainstay in cancer therapy and many immune-related diseases. However, a main concern for patients taking CTX at higher doses or for long time periods is its side effects, which include haemorrhagic cystitis[2], nephrotoxicity[3] and cardiotoxicity[4]. Moreover, many patients also suffer from severe gut injury, including intestinal inflammation, disrupted intestinal barrier and gut dysbiosis[5, 6]. Therefore, it is critical to find novel agents to alleviate the toxicity induced by CTX.

The normal function of the gastrointestinal (GI) tract is pivotal for proper absorption of nutrients, whereas alterations of the GI tract result in severe defects in intestinal barrier and potentially to GI diseases[7, 8]. The intestinal epithelial cells, which represent a physical barrier, are closely connected by tight junctions (TJs), which regulate the paracellular transport of molecules. The complex interactions among TJ proteins preserve the integrity of intestinal barrier and prevent gut permeability[9]. Interestingly, a "leaky" gut can robustly activate immune cells to secrete inflammatory cytokines, which in turn will further increase the gut permeability[10]. Gut hyperpermeability can promote pathogens or toxins to diffuse into the systemic circulation and have been shown to correlate with various non-intestinal diseases, such as diabetes, obesity, Alzheimer's disease and allergies[11-14]. Furthermore, commensal microorganisms cohabiting in the GI tract can also compromise the gut barrier function via promoting mucosal inflammatory responses and disassembling TJs[15, 16]. It is reported that the intestinal microbial homeostasis is highly influenced by various environmental stressors, such as diets, antibiotics, inflammatory stimuli, and certain drugs[17]. Thus, keeping the balance of luminal microflora is critical to maintain the gut barrier integrity.

Epigallocatechin-3-gallate (EGCG) is the most biologically active and abundant component of tea polyphenols. Extensive evidence has documented that EGCG exhibits diverse beneficial functions, including anti-oxidant, anti-tumor, anti-aging, and

anti-inflammation[18-20]. Furthermore, EGCG has also been reported to alleviate the gut injury through multiple mechanisms, such as alleviating the inflammation response[21], maintaining Th1/Th2 balance[22] and activating Nrf2 signal pathway[23]. However, the protective effect of EGCG to improve CTX-induced GI damage remains unknown. In this study, we evaluated whether EGCG could mitigate the intestinal adverse effects induced by CTX, by assessing intestinal morphology, barrier function, pro-inflammatory cytokine secretion, and flora compositions in CTX-treated mice.

2. Materials and Methods:

2.1 Materials and Chemicals

EGCG (purity≥98%) was purchased from Solarbio (Beijing, China). CTX (purity≥98%) was purchased from Aladdin (Shanghai, China). The Elisa kits for IL-10, IL-21, TNFα were purchased from Multisciences Biotech (Hangzhou, China). The ReverTra Ace qPCR RT master mix and the SYBR Green Realtime PCR master mix were purchased from TOYOBO (Shanghai, China). The designed oligo nucleotide primers were generated by Sangon Biotech (Shanghai, China). The RIPA lysis buffer, Halt protease inhibitor cocktail, 5×SDS-PAGE sample loading buffer, BSA, Bradford protein assay kit and ECL Plus Ultra Sensitive kit were purchased from Phygene (Haixi, China). The PVDF membranes and the fluorescein isothiocyanate-dextran (FITC-Dextran) were purchased from MilliporeSigma (Burlington, MA, USA). The prestained protein ladder and TRIzol™ Reagent were purchased from Thermo Fisher Scientific (Waltham, MA, USA). The Occludin (Cat#13409), Claudin-1 (Cat#13050), ZO-1 (Cat#21773) and GAPDH (Cat#60004) antibodies were purchased from Proteintech™ (Wuhan, China). The total antioxidant capacity (T-AOC) assay kit, malondialdehyde (MDA) colorimetric assay kit, catalase (CAT) colorimetric assay kit, superoxide dismutase (SOD) colorimetric assay kit and glutathione peroxidase (GSH-PX) colorimetric assay kit were purchased from JianCheng Bioengineering Institute (Nanjing, China). The acetic, propionic, isobutyric, butyric, isovaleric, and valeric acids standards were purchased from CNW Technologies (Duesseldorf, Germany).

2.2 Animal Studies

The animal studies were approved by the Laboratory Animal Center of Zhejiang Agricultural and Forestry University. Four-week old ICR male mice were purchased from the Shanghai SLAC Laboratory Animal Company (Shanghai, China) and maintained under semi-specific pathogen-free (SPF) conditions, housed under a 12 h light cycle and fed with autoclaved chow diet. Briefly, after 2 weeks adaptation, mice were divided randomly into 2 groups: CTX-treated group (n=18) and vehicle-treated group (n=12). Mice in CTX group were injected intraperitoneally with 50 mg/kg/d CTX for 5 days, while the vehicle-treated group were injected with PBS. On the 6th day, CTX-treated mice were further randomized into 3 groups (n=6/group), and orally gavaged daily with water (CTX group), low dose (20 mg/kg/d) EGCG [CTX+E(L)], or a high dose (40 mg/kg/d) EGCG [CTX+E(L)] for additional 25 days (Figure 1A). Moreover, on day 6, the non-treated mice were separated randomly into the control group (Ctrl) and high dose (40 mg/kg/d) EGCG group [E(H)] (n=6/group). The body weight was measured every 5 days. Fresh feces were collected on the 29th day and stored in -80°C until gut microbial and the short chain fatty acids (SCFAs) analysis. On the 30th day, mice were fasted 4 h for the gut permeability analysis. After blood collecting, mice were euthanized and small intestine was carefully dissected, washed with PBS and then, half was immersed in 4% (w/v) paraformaldehyde for histochemistry analysis, and the other were stored in -80°C freezer. The spleen and thymus were also collected and weighed.

2.3 Histological analysis

Following euthanasia, the intestine tissues (n=6/group) were fixed in 4% (w/v) paraformaldehyde paraffin embedded, sectioned and stained with hematoxylin and eosin (H&E). Images at x20 and x100 magnification were taken by light microscopy (Olympus BX-41, Tokyo, Japan). Image J software was used to measure the villi height and crypt depth.

2.4 Mouse gut permeability analysis

On the last day, mice (n=6/group) were fasted for 4h. Then, mice were orally gavaged with fluorescein isothiocyanate conjugated dextran (50 mg per 100 g body weight). After 2 h, blood was collected and serum was separated[24]. The fluorescence intensity (excitation, 490nm; emission, 520nm) was measured using the Synergy H1 microplate reader (Biotek, VT, USA).

2.5 Western blot

Frozen small intestine tissue samples (n=6/group) were thawed, homogenized and lysed with RIPA lysis buffer over ice, and the protein content was measured by the Bradford protein assay kit. Aliquots of total fractions containing 20-40 μg protein were separated using 10% (w/v) polyacrylamide gel electrophoresis and were electroblotted to PVDF membranes. The membranes were blocked and probed overnight with primary antibodies (1:1000 dilution): ZO-1, Occludin and Claudin-1. GAPDH was used as the loading control. After incubation in the presence of the secondary antibody (HRP-conjugated; 1:5000 dilution) for 1 h at room temperature, the immunoblots were developed and visualized using the MiniChemi™ System (SageCreation, Beijing, China).

2.6 ELISA

Frozen small intestinal tissue samples (n=6/group) were thawed, homogenized over ice in PBS, centrifuged and the supernatant was obtained. The levels of IL-10, IL-21 and TNFα in the supernatant were measured by Elisa kits, following the manufacturer's instructions (Multisciences Biotech, Hangzhou, China). The optical density was measured using the Synergy H1 microplate reader (Biotek, VT, USA).

2.7 RNA extraction and qRT-PCR analysis

Total RNA of the homogenized small intestine tissue samples (n=6/group) were extracted using the TRIzol™ Reagent on ice and purity and quantity were determined by the Nanodrop™ One spectrophotometer (Thermo Fisher Scientific, MA, USA). cDNA was obtained using the ReverTra Ace qPCR RT master mix with the Veriti

thermal cycler (Thermo Fisher Scientific, MA, USA). Afterwards, the qPCR was performed by using the SYBR Green Realtime PCR master mix and were monitored by using the StepOne Realtime PCR system (Thermo Fisher Scientific, MA, USA). Data were analyzed by $2^{-\Delta\Delta Ct}$ method. Primer used are shown in Table1[25-29].

2.8 Redox status analysis

Small intestine samples (n=6/group) were homogenized over ice with PBS and then centrifuged at 12,000 rpm at 4°C for 15 min. Supernatants were obtained and the levels of T-AOC, MDA, and enzymatic activity of CAT, GSH-PX, SOD were tested according to the manufacturer's guidelines. Protein content were determined using the Bradford protein assay kit.

2.9 Gut microbe 16S rRNA sequencing

Total DNA was isolated from mouse feces (n=4/group) using E.Z.N.A.® Soil DNA Kit (Omega Bio-tek, GA, USA). The V3–V4 regions of bacterial 16S rRNA gene was amplified by ABI GeneAmp® PCR (Thermo Fisher Scientific, MA, USA), with universal primers 338 F (5′-ACTCCTACGGGAGGCAGCAG-3′) and 806R (5′-GGACTACHVGGGTWTCTAAT-3′). Subsequently, duplicate PCR products were excised from a 2 % (w/v) agarose gel and purified by AxyPrep DNA Gel Extraction Kit (Axygen Biosciences, CA, USA) and quantified using QuantiFluor™-ST (Promega, WI, USA) according to the manufacturer's protocol. Sequencing library was built up using TruSeq™ DNA Sample Prep Kit and then sequenced by an Illumina MiSeq platform (Illumina, SD, USA).

2.10   Bioinformatic analysis

Raw fastq files were quality-filtered by Trimmomatic and merged by FLASH. Then the high-quality sequences were clustered into operational taxonomic units (OTUs) according to a 97 % similarity cutoff using the USEARCH (version 7.1 http://drive5.com/uparse/) with a novel 'greedy' algorithm that performs chimera filtering and OTU clustering simultaneously. The taxonomy of each 16S rRNA gene

sequence was analyzed by RDP Classifier algorithm (http://rdp.cme.msu.edu/). For α-diversity, Chao, Ace and Shannon, Simpson were performed respectively to analyze community richness and diversity. Variation in community composition (β-diversity) was measured by calculating the principal component analysis (PCA). Partial Least Squares Discriminant analysis (PLS-DA) was performed to analyze the differences within groups. The linear discriminant analysis (LDA) and LDA effect size (LEfSe) methods were applied to compare and visualize different taxa microbes among groups based on Galaxy Online Analysis Platform (http://huttenhower. sph.harvard.edu/galaxy/).

2.11   Short chain fatty acids levels

Fecal short chain fatty acids (SCFAs) content was analyzed as previously described[30]. Briefly, fecal samples (n=6/group) were mixed with phosphoric acid (0.5% v/v) solution, homogenized, vortexed and ultrasonicated for 10 min. After centrifuged at 12,000 rpm, 4°C for 10 min, supernatants were collected. Then, supernatants were mixed with 2-methylvaleric (the internal standard), vortexed, ultrasonicated and filtered for analysis. Agilent 7890B gas chromatograph coupled to a 7000D mass spectrometer with a DB-FFAP column (30 m length × 0.25 mm diameter × 0.25 µm film thickness, J&W Scientific, USA) was employed for GC-MS/MS analysis of SCFAs. The initial oven temperature was set at 90°C and then increased to 200°C. Helium was used as carrier gas, at a flow rate of 1.2 mL/min. Standard acetic acid, propionic acid, butyric acid, isobutyric acid, valeric acid and isovaleric acid were used to establish the standard plots.

2.12 Statistical analysis

All results are expressed as Mean ± SD. One-way analysis of variance (ANOVA) and Turkey post hoc tests were performed to evaluate the differences among groups (SPSS 20.0 software, Chicago, IL). $p < 0.05$ was regarded as being statistically significant.

3. Results:

3.1 EGCG accelerates recovery of body weight loss induced by cyclophosphamide.

To evaluate the capacity of EGCG to attenuate the gut injury induced by CTX in mice, we first treated mice with CTX for 5 days to induce gut injury, and then we administered EGCG, at two doses, for an additional 25 days (Figure 1A). Treatment with CTX for 5 days led to a significant weight loss that was evident starting on day 10 following the start of the treatment. Daily administration of EGCG, at both low (20mg/kg/d) and high (40mg/kg/d) doses, which started on day 6, after the last dose of CTX, enhanced the recovery of body weight loss induced by CTX to some extent, which was significant at day 30 (Figure 1B). Of note, the body weights in the Ctrl and EGCG [E(H)] alone groups (both not receiving CTX) were comparable throughout the experimental period (Figure 1B).

3.2 EGCG protects intestine structure in cyclophosphamide treated mice

To evaluate whether EGCG presented a beneficial role on the gut barrier integrity in CTX-treated mice, we investigated intestine morphology by H&E staining. As shown in Figure 1C, the intestine tissue of vehicle control and EGCG groups were well-structured, with tight and orderly arranged villi and short crypts. In contrast, the intestine mucosa of CTX-treated mice appeared ulcerated, and the intestine structure was seriously damaged. Villi were out of shape and bigger space were observed between the adjacent ones. EGCG treatment improved intestinal morphology with both the villi and crypt structures returning to its normal appearance. These observations were evaluated by analyzing the villi height and crypt depth as well as calculating the villus/crypt ratio. While CTX significantly shortened the villi height to 270.5±21.1 μm ($p < 0.01$) and deepened the crypt to 139.1±15.8 μm ($p < 0.05$), largely decreased the villus/crypt ratio to 1.94 ($p < 0.01$), treatment of EGCG 40 mg/kg/d ($p < 0.05$) restored villi height and crypt depth to values comparable to those observed in control mice (Figure 1C).

3.3 EGCG improves intestine permeability damaged by cyclophosphamide

We next evaluated the effect of EGCG on CTX-induced intestinal permeabilization, by measuring the intestinal transport of FITC-dextran after 30 days in the various experimental groups. CTX treatment increased the intestine permeability by 4.94 fold compared to the control group ($p < 0.01$). CTX mice treated with EGCG 40 mg/kg/d showed a robust reduction in intestinal permeabilization (2.44 fold versus control), being significant different to that of CTX group (Figure 2A).

Mechanically, we explored whether EGCG could affect the expression of tight junction proteins, which play a key role in keeping intestine barrier intactness. As shown in Figure 2B, administration of CTX reduced ZO-1, Occludin and Claudin-1 protein expression ($p < 0.01$, $p < 0.05$, and $p < 0.05$, respectively), whereas treatment with EGCG after CTX administration (CTXE group) improved the expression of ZO-1, Occludin and Claudin-1, restoring the levels to those observed in the Ctrl or EGCG alone groups (Figure 2B).

3.4 EGCG reduces the levels of inflammatory cytokines enhanced by cyclophosphamide

Given that inflammatory cytokines can affect the intestinal mucosal immunity, we examined the effect of EGCG on the secretion of inflammatory cytokines in CTX-treated mice. Treatment with CTX significantly upregulated the levels of IL-10, IL-21 and TNFα ($p < 0.01$, $p < 0.01$, and $p < 0.05$, respectively), which were ameliorated by EGCG at both low and high doses (Figure 3). For instance, IL-21 levels in CTX group were around 102.6±8.5 pg/ml, and were reduced to 80.7±10.2 pg/ml and 75.9±6.3 pg/ml, after treatment with of low and high dose of EGCG, respectively. Similar findings were observed by determining the mRNA levels of these cytokines. For example, CTX group displayed higher IL-10, IL-21 and TNFα mRNA levels ($p < 0.01$), compared to the Ctrl group, whereas these levels decreased markedly after treatment with EGCG. Of note, compared with the CTX group (2.5±0.4 fold over Ctrl), EGCG intervention, at both low and high doses, significantly reduced the IL-21 mRNA levels to 1.6±0.2 and

1.3±0.3 fold over Ctrl, respectively (Figure 3).

Because CTX is well-known for its immunosuppressive effects[31], we determined the spleen and thymus index, by assessing their weights at euthanasia, to explore the effect of EGCG on the immunity system organs in the CTX-treated mice. Compared to the Ctrl group, CTX reduced the spleen index to 0.21% (Figure 4). Treatment with EGCG, high dose in particular, improved the spleen index to 0.32%, significantly higher than that of the CTX-treated mice (p < 0.05). Meanwhile, the thymus index was reduced to 0.13% in the CTX group, and it was restored to the normal level with the supplementation of EGCG. For instance, the thymus index of high dose EGCG [CTX + E(H)] group was 0.16%, higher than the ones of CTX group (Figure 4).

3.5 EGCG mitigates the increase in reactive oxygen species induced by cyclophosphamide

We next evaluated the effect of EGCG on CTX-induced increase in reactive oxygen species, by measuring the malondialdehyde (MDA) levels, as a marker of lipid peroxidation, and the total antioxidant capacity (T-AOC) in the intestine tissue. Compared with the control group, CTX induced oxidative stress in the intestine tissue, as evidenced by a decreased T-AOC and an increased MDA levels (p < 0.01; Figure 5A). Supplementation with high dose EGCG increased the T-AOC (p < 0.05), and reduced MDA levels (p < 0.01). Moreover, CTX treatment decreased the enzymatic activity and mRNA expression levels of the key antioxidant enzymes CAT, SOD and GSH-PX (p < 0.01; Figure 5B). On the other hand, compared to the CTX group, EGCG restored the activity and and mRNA expression levels of CAT, SOD and GSH-PX to those observed in the control group. For example, CTX reduced CAT activity to 38.6± 1.6 U/g prot, which was increased by EGCG high dose to 76.2± 4.7 U/g prot (p < 0.01), to comparable activity levels observed in control group (92.6± 6.4 U/g prot). These results suggest that EGCG mitigates the oxidative stress induced by CTX.

3.6 EGCG modulates the taxonomic composition in cyclophosphamide treated

mice

Given that the microbiota is a key factor closely associated with the intestinal mucosal immunity, we then performed 16S rRNA sequencing to evaluate the microflora overall structure among the various experimental groups. To examine whether CTX could affect the richness and diversity of the microbial community, we initially assessed the α-diversity among groups. As shown by the Shannon and Simpson diversity indices, treatment with CTX increased α-diversity compared with Ctrl group (Figure 6). CTX mice treated with EGCG had no major effect on α-diversity compared to those only treated with CTX. Moreover, no major changes in the Ace and Chao1 indices were observed, which suggest that the community richness was kept relatively stable among all groups.

We next compared the spatial diversity of the bacterial genus among groups, represented in a Venn diagram (Figure 7A). The spatial diversity revealed that 392 operational taxonomic units (OTUs) out of the total OTUs were overlapped among all the groups. Furthermore, there were 7, 15, 6 and 4 OTUs out of the total that were unique to the Ctrl, CTX, CTXE, E groups, respectively.

To confirm the specific changes of the microbial community, we analyzed the taxonomic components for the various groups at the phylum and family levels. At phylum level (Figure 7B), Firmicutes and Bacteroidetes, two major phyla present in the intestine, were the two predominant phyla of all groups, accounting for about 90% of the total bacteria. Compared with the control group, CTX treatment increased the abundance levels of Firmicutes, whereas reducing the levels of Bacteroidetes. This change was clearly observed by calculating the Firmicutes/Bacteroidetes ratio (Figure 7C). The Firmicutes/Bacteroidetes ratio reached to 7.4 in CTX group, about 3 times higher than that of the control group ($p < 0.05$). Notably, EGCG itself had no major effect on the fecal bacteria abundance. However, EGCG intervention reduced, to some degree, the Firmicutes/Bacteroidetes ratio affected by CTX (CTXE group), by increasing the levels of Bacteroidetes (Figure 7B). Desulfobacterota and Patescibacteria constituted the next predominant phylum and were higher in the CTX group, and EGCG intervention decreased the abundance of these two phyla.

At the family level, CTX induced the upregulation of the relative abundance of Lactobacillaceae, Lachnospiraceae, Desulfovibrionaceae and Saccharimonadaceae, as well as decreased the content of Muribaculaceae and Erysipelotrichaceae (Figure 7D). CTX mice treated with EGCG presented similar levels of the above-mentioned bacteria families to the mice in the control group. Thus, CTX treatments disturbs the balance of the gut microflora, while EGCG appears to, in part, restore the intestinal microbiota dysbiosis induced by CTX.

3.7 EGCG regulates the specific phylotypes of the gut microbiome in cyclophosphamide treated mice

Based on the differences in microbial community composition among groups, we next performed a principal component analysis (PCA) to define the similarity of species diversity among groups on operational taxonomic unit (OTU) level (Figure 8A). Most samples of control, EGCG and CTXE groups shared relatively close similarity, while CTX samples induced significant microbial community changes. Similar observations were obtained using the partial least squares discriminant analysis (PLS-DA). As shown in Figure 8B, microbial samples clustered by each treatment group and apparent separation existed between CTX and other groups.

Finally, we aimed to identify some key species of gut microbiota that are different among groups by performing the LEfSe analysis (Figure 8C). LDA results showed 11 discriminative features in the control group (LDA $>$ 2, p $<$ 0.05), and the major microbiotas including s_uncultured_bacterium_g_norank_f_Muribaculaceae, s_Ralstonia_pickettii and f_Burkholderiaceae. In CTX group, 14 primary microorganisms were remarkable different, such as s__unclassified_g__Candidatus_Soleaferrea and g__Candidatus_Soleaferrea, etc (Figure 8C). Besides, 9 prominent different features were observed in the EGCG group, such as p__Bacteroidota, c__Bacteroidia, and o__Bacteroidales etc. Finally, though only s_unclassified_f_Eggerthellaceae and g__unclassified_f__Eggerthellaceae were substantially different in the CTXE group, it is still possible that EGCG could alter the key phylotypes of the gut microbiome modified by CTX to a large extent.

3.8 EGCG increased the level of SCFAs in the feces reduced by cyclophosphamide

Given that SCFAs are main end products produced by gut microbiota, we determined the effect of EGCG on SCFAs in fecal samples of CTX-treated mice. As presented in Figure 9, CTX treatment reduced the levels of acetic, propionic, isobutyric, butyric, isovaleric and valeric acids, compared with the control group. Following administration with EGCG, the level of these SCFAs increased, although in varying degrees. Compared with the CTX group, EGCG increased the levels of acetic and butyric acids ($p < 0.01$, $p < 0.05$ and $p < 0.01$, respectively). However, no significant differences were observed in propionic, isobutyric, isovaleric and valeric acids between the CTX group and the CTXE group (Figure 9).

4. Discussion:

Even though CTX is one of the oldest anticancer drugs, dating back to 1959, it is still commonly used in treating various tumor-types[1]. Besides its anticancer use, CTX is also administered as an immunosuppressant, to treat autoimmune and immune-mediated diseases, such as lupus nephritis, rheumatoid arthritis, and multiple sclerosis[32]. Unfortunately, the chronic use of CTX presents some adverse effects, including haemorrhagic cystitis[2], hepatic damage[33], cardio toxicity[4] and GI impairments[6]. In this study, we evaluated the beneficial effect of EGCG to recover from CTX-induced GI toxicity. While CTX-treated mice showed intestine damage, inflammation and immune organ atrophy, these symptoms were favorably alleviated by EGCG.

The GI tract is a main organ system affected by CTX's toxicity. Specifically, the intestine injury caused by CTX is usually manifested as impaired intestinal structure, disrupted intestinal mucosal immunity, reduced expression level of tight junction proteins, increased oxidative stress and altered gut microbiota composition among the most significant [6, 34, 35]. Anatomically, the GI tract is composed by the lumen, mucus

layer and epithelial cells that form a dynamic, permeable barrier[36]. It is responsible for the selective absorption of nutrients, while restricting the entrance of pathogens and other toxins. We observed that even after 25 days following CTX challenge, CTX-treated mice presented damaged mucosal layer, deformed villi and irregular crypt[37]. Moreover, CTX substantially increased the gut permeability when compared with the vehicle-treated mice. Consistent with our findings, multiple studies revealed that CTX affects the GI tract, causes leakage of the gut barrier, induces inflammatory stress and gut dysbiosis[38, 39]. Therefore, there is urgent need to evaluate agents that can ameliorate CTX's adverse effects.

EGCG is a tea-derived polyphenol with multiple health benefits[40, 41], like protecting the GI tract[21-23]. In this study, we document that treatment with EGCG accelerates the recovery of the intestinal barrier damage triggered by CTX. The beneficial effects of EGCG were associated with its ability to alleviate the inflammation response, strengthen the tight junctions and regulate the gut microbial structure. Consistent with our findings, EGCG has been shown to inhibit bacterial translocation and enhance the intestinal barrier function by stimulating the secretion of antimicrobial peptides, porcine β-defensins 1 and 2 (pBD-1 and 2) in porcine jejunal epithelial cell line IPEC-J2[42]. EGCG could also protect against the intestinal permeability alterations induced by indomethacin in Caco-2 cells[43].

As is the case with many polyphenols, the systemic bioavailability of EGCG is low[44]. It is known that EGCG is extensively metabolized after oral administration, and it can be absorbed in the intestine and metabolized by intestinal gut microbiota. Regarding its metabolism, EGCG is hydrolyzed to EGC and gallic acid, with EGC being then converted to 5-(3,5-dihydroxyphenyl)-4-hydroxyvaleric acid[45]. Although its systemic levels are low, EGCG can accumulate in the intestinal mucosa in sufficient amounts to exert a biological action[46]. A limitation of our study is that we have not assessed the levels of EGCG metabolites. It is likely that metabolites of EGCG may also contribute to the observed protective effect against CTX-induced intestinal damage.

At the cellular level, the intestinal barrier is controlled by the TJs located between the epithelial cells, which limit the paracellular transport of bacteria and bacterial products. Multiple proteins are involved in the assembly of these TJs, like Occludin and Claudin-1, two of the membrane spanning proteins. These proteins bind with ZO-1, and connect to the actin microfilaments intracellularly[47]. Treatment with EGCG increased the expression levels of ZO-1, Occludin and Claudin-1, which were largely reduced by CTX. These results suggest that EGCG could repair the damaged gut barrier in CTX-induced mice, in part, by modulating TJ proteins.

The dysfunction of the intestinal barrier is also the causal or complicating factor in the pathology of intestinal inflammation[48]. Certain interleukins and tumor necrosis factor are primary pro-inflammatory cytokines, mainly secreted by the immune cells, such as B cells, T cells and NK cells[49]. CTX stimulated the release of IL-21 and TNFα, two of the important pro-inflammatory cytokines, to a similar degree of what was shown in other studies[5, 6, 37]. Meanwhile, it is worth noting that the levels of IL-10, which is regarded as an anti-inflammatory cytokine, was also significantly increased with CTX treatment. Interestingly, IL-10 has been shown to also exert pro-inflammatory properties, and this dual function is still poorly understood[50-52]. EGCG reduced the levels of these cytokines, suggesting that EGCG is able to mitigate against the inflammatory stress induced by CTX. Consistent to our findings, EGCG has been documented to down-regulate the levels of inflammatory cytokines in the GI tract in mouse models of colitis as well as in lipopolysaccharide-stimulated human intestinal epithelial cells [53, 54], suggesting that the anti-inflammatory effect of EGCG may account for the beneficial effect of EGCG improving intestinal damage induced by CTX.

The aberrant generation of reactive oxygen species is a primary inflammatory stimulus and plays a critical role in initiating intestinal injury[55-57]. Interestingly, CTX is known to induce reactive oxygen species *in vivo*[58-60]. In agreement, we observed that CTX induced reactive oxygen species at the intestine level. The increase in reactive oxygen species was mitigated by treatment with EGCG, mainly through the regulation of the activity and expression levels of the major endogenous enzymatic antioxidants,

such as CAT, SOD and GSH-PX. Consistent with our findings, EGCG was shown to prevent the gut oxidative injury of heat-stressed broilers through increasing the activities of GSH-PX, SOD and CAT, and reducing the MDA level[21].

The GI tract hosts millions of commensal microorganisms, which closely interact with the epithelial and immune cells[61]. Under normal circumstances, intact intestinal barrier will thwart the luminal bacteria or bacterial products access into the systemic circulation. While when leaky gut occurred, the harmful microorganisms will be directly into the systemic circulation, and is increasingly considered as a critical determinant in the development of multiple diseases[11-14]. Therefore, keeping microbial balance is recognized as very important for overall health. By means of the α-diversity analysis, we observed no significant differences in the community richness among groups, with EGCG having no major changes in the community diversity compared to CTX.

Given that the structural composition of the gut microbiota may change after drug manipulation[62], we then compared the community abundance of the predominant gut microbiota from high taxonomic levels. At the phylum level, Firmicutes and Bacteroidetes were the two prevalent phyla in all groups, representing over 90% of the community. CTX notably enhanced the Firmicutes/Bacteroidetes ratio, which is consistent to what was observed in other studies where CTX enhanced the proliferation of Proteobacteria and Firmicutes altering the composition of the microbial community[38, 63]. Interestingly, an increase of Firmicutes/Bacteroidetes ratio is frequently observed related to obesity and other diseases[64], such as inflammatory bowel disease (IBD), and ulcerative colitis (UC) [65-67]. For instance, in a colitis model in rats, an enhanced Firmicutes/Bacteroidetes ratio was observed, and the colonic injury was reported to be negatively correlated with Firmicutes[68]. In our study, EGCG treatment increased the abundance of Bacteroidetes, one of the most important SCFAs producers[69], and reduced the Firmicutes/Bacteroidetes ratio in CTX-treated mice. Consistent to our findings, EGCG was found to significantly reduce the Firmicutes/Bacteroidetes ratio in mice fed a high-fat diet[70].

SCFAs are the major metabolites of gut microflora, and shape the gut environment. Acetate, propionate and butyrate dominate about 90%-95% of the total SCFAs contents. It is well-established that SCFAs play a vital role over mucosal maintenance and integrity through facilitating the tight junction proteins assembly, fueling the growth of the epithelial cells, and alleviating the gut inflammation[71]. Tea polyphenols are reported would promote SCFAs production [72, 73]. In agreement, our results showed that EGCG is highly effective in generating SCFAs, in particular, acetic and butyric acids, which may explain the thus attenuating the gut environment damage induced by CTX.

At family level, CTX increased the relative abundance of Lactobacillaceae, Lachnospiraceae, Desulfovibrionaceae and reduced the level of Muribaculaceae. Lactobacillaceae and Lachnospiraceae are the members of phylum Firmucutes, which are involved in the microbiota-immunity symbiotic loop, associated with several diseases[74, 75]. Female mice with systemic lupus erythematosus-prone symptoms are correlated with Lachnospiraceae abundance[76]. Desulfovibrionaceae is one of the endotoxin-producing opportunistic pathogens, involved in gut barrier disruption[77, 78]. In CTX-treated mice, EGCG reduced the levels of Lachnospiraceae and Desulfovibrionaceae, while increased the level of Muribaculaceae, which is recognized as a dominant bacterial taxonomic family within the Bacteroidota phylum of murine microbiota[79, 80].

Based on the diverse community composition among groups, the results of PCA and PLS-DA further proved the community difference among groups. Using the LEfSe analysis, we identified key phylotypes of gut microbiota among groups. It is interesting to note that the dominant microorganism of CTXE group was the Eggerthellaceae, which has been reported to metabolize secondary plant compounds[81], especially polyphenols like ellagic acid[82], daidzein[83], and resveratrol[84]. Moreover, Eggerthellaceae has been shown to cleave the heterocyclic C-ring of both (-)-epicatechin and (+)-catechin, and transform catechins into 1-(3,4-dihydroxyphenyl)-3-(2,4,6-trihydroxyphenyl)propan-2-ol[85]. In summary, EGCG can strongly modulate

intestinal microbiome. Further investigation about the role of gut microorganisms on EGCG and other metabolites as well as the interactions among EGCG, the gut microbiotas, and the intestinal barrier function are warranted to deeply elucidate the protective effect of EGCG on the GI tract.

5. Conclusions

The present study indicates that EGCG alleviates the GI tract damage induced by CTX. EGCG's beneficial actions are mediated, in part, via its effect mitigating intestine mucosa inflammation, protecting the gut barrier, and maintaining gut homeostasis. Moreover, EGCG restores the microflora homeostasis altered by CTX via modulating the composition of the microbial community and restoring the SCFAs production. In conclusion, EGCG may function as an effective bioactive to minimize CTX-induced GI tract toxicity.

CRediT Author contributions: Ran Wei: Conceptualization, Methodology, Visualization, Investigation, Writing- Original draft preparation, Reviewing and Editing, Funding acquisition. **Xingquan Liu and Yuefei Wang**: Methodology and Investigation, Reviewing and Editing. **Junjie Dong**: Reviewing and Editing, Funding acquisition. **Fenghua Wu**: Investigation, Reviewing and Editing. **Gerardo G. Mackenzie**: Conceptualization, Writing-Reviewing and Editing, Funding acquisition. **Zhucheng Su**: Conceptualization, Writing-Reviewing and Editing, Funding acquisition.

Conflicts of Interest: The authors declare no conflict of interest.

References

1.   A. Emadi, R. J. Jones and R. A. Brodsky, Cyclophosphamide and cancer: golden anniversary, *Nat Rev Clin Oncol*, 2009, **6**, 638-647.

2.   T. J. Stillwell and R. C. Benson, Jr., Cyclophosphamide-induced hemorrhagic cystitis. A review of 100 patients, *Cancer*, 1988, **61**, 451-457.

3.   M. U. Rehman, M. Tahir, F. Ali, W. Qamar, A. Lateef, R. Khan, A. Quaiyoom, O. H. Oday and S. Sultana, Cyclophosphamide-induced nephrotoxicity, genotoxicity, and damage in kidney genomic DNA of Swiss albino mice: the protective effect of Ellagic acid, *Mol Cell Biochem*, 2012, **365**, 119-127.

4.   M. A. Goldberg, J. H. Antin, E. C. Guinan and J. M. Rappeport, Cyclophosphamide cardiotoxicity: an analysis of dosing as a risk factor, *Blood*, 1986, **68**, 1114-1118.

5.   S. I. Lee and K. S. Kang, Function of capric acid in cyclophosphamide-induced intestinal inflammation, oxidative stress, and barrier function in pigs, *Sci Rep*, 2017, **7**, 16530.

6.   H. Shi, Y. Chang, Y. Gao, X. Wang, X. Chen, Y. Wang, C. Xue and Q. Tang, Dietary fucoidan of Acaudina molpadioides alters gut microbiota and mitigates intestinal mucosal injury induced by cyclophosphamide, *Food Funct*, 2017, **8**, 3383-3393.

7.   M. A. McGuckin, R. Eri, L. A. Simms, T. H. Florin and G. Radford-Smith, Intestinal barrier dysfunction in inflammatory bowel diseases, *Inflamm Bowel Dis*, 2009, **15**, 100-113.

8.   D. Cardoso-Silva, D. Delbue, A. Itzlinger, R. Moerkens, S. Withoff, F. Branchi and M. Schumann, Intestinal Barrier Function in Gluten-Related Disorders, *Nutrients*, 2019, **11**.

9.   M. A. Odenwald and J. R. Turner, The intestinal epithelial barrier: a therapeutic target?, *Nat Rev Gastroenterol Hepatol*, 2017, **14**, 9-21.

10.   C. W. Teshima, L. A. Dieleman and J. B. Meddings, Abnormal intestinal permeability in Crohn's disease pathogenesis, *Ann N Y Acad Sci*, 2012, **1258**, 159-165.

11.   E. Patterson, P. M. Ryan, J. F. Cryan, T. G. Dinan, R. P. Ross, G. F. Fitzgerald and C. Stanton, Gut microbiota, obesity and diabetes, *Postgrad Med J*, 2016, **92**, 286-300.

12.   C. Jiang, G. Li, P. Huang, Z. Liu and B. Zhao, The Gut Microbiota and Alzheimer's Disease, *J Alzheimers Dis*, 2017, **58**, 1-15.

13.   S. V. Lynch, Gut Microbiota and Allergic Disease. New Insights, *Ann Am Thorac Soc*, 2016, **13 Suppl 1**, S51-54.

14.   C. Maynard and D. Weinkove, The Gut Microbiota and Ageing, *Subcell Biochem*, 2018, **90**, 351-371.

15.   H. Tilg, N. Zmora, T. E. Adolph and E. Elinav, The intestinal microbiota fuelling metabolic inflammation, *Nat Rev Immunol*, 2020, **20**, 40-54.

16.   B. Allam-Ndoul, S. Castonguay-Paradis and A. Veilleux, Gut Microbiota and Intestinal Trans-Epithelial Permeability, *Int J Mol Sci*, 2020, **21**.

17.   B. Das and G. B. Nair, Homeostasis and dysbiosis of the gut microbiome in health and disease, *J Biosci*, 2019, **44**.

18.   D. G. Nagle, D. Ferreira and Y. D. Zhou, Epigallocatechin-3-gallate (EGCG): chemical and biomedical perspectives, *Phytochemistry*, 2006, **67**, 1849-1855.

19.   R. Wei, L. Mao, P. Xu, X. Zheng, R. M. Hackman, G. G. Mackenzie and Y. Wang, Suppressing glucose metabolism with epigallocatechin-3-gallate (EGCG) reduces breast cancer cell growth in preclinical models, *Food Funct*, 2018, **9**, 5682-5696.

20.   K. Kawai, N. H. Tsuno, J. Kitayama, Y. Okaji, K. Yazawa, M. Asakage, N. Hori, T. Watanabe, K. Takahashi and H. Nagawa, Epigallocatechin gallate attenuates adhesion and migration of CD8+ T cells by binding to CD11b, *J Allergy Clin Immunol*, 2004, **113**, 1211-1217.

21.   J. Song, X. Lei, J. Luo, N. Everaert, G. Zhao, J. Wen and Y. Yang, The effect of Epigallocatechin-3-gallate on small intestinal morphology, antioxidant capacity and anti-inflammatory effect in heat-stressed broilers, *J Anim Physiol Anim Nutr (Berl)*, 2019, **103**, 1030-1038.

22.   X. Bing, L. Xuelei, D. Wanwei, L. Linlang and C. Keyan, EGCG Maintains Th1/Th2 Balance and Mitigates Ulcerative Colitis Induced by Dextran Sulfate Sodium through TLR4/MyD88/NF-kappaB Signaling Pathway in Rats, *Can J Gastroenterol Hepatol*, 2017, **2017**, 3057268.

23.   L. W. Xie, S. Cai, T. S. Zhao, M. Li and Y. Tian, Green tea derivative (-)-epigallocatechin-3-gallate (EGCG) confers protection against ionizing radiation-induced intestinal epithelial cell death both in vitro and in vivo, *Free Radic Biol Med*, 2020, **161**, 175-186.

24.   J. W. Ruan, S. Statt, C. T. Huang, Y. T. Tsai, C. C. Kuo, H. L. Chan, Y. C. Liao, T. H. Tan and C. Y. Kao, Dual-specificity phosphatase 6 deficiency regulates gut microbiome and transcriptome response against diet-induced obesity in mice, *Nat Microbiol*, 2016, **2**, 16220.

25.   N. Chiba, A. Masuda, Y. Yoshikai and T. Matsuguchi, Ceramide inhibits LPS-induced production of IL-5, IL-10, and IL-13 from mast cells, *J Cell Physiol*, 2007, **213**, 126-136.

26.   T. Zhang, C. Ding, M. Zhao, X. Dai, J. Yang, Y. Li, L. Gu, Y. Wei, J. Gong, W. Zhu, N. Li and J. Li, Sodium Butyrate Reduces Colitogenic Immunoglobulin A-Coated Bacteria and Modifies the Composition of Microbiota in IL-10 Deficient Mice, *Nutrients*, 2016, **8**.

27.   M. Ying, Q. Yu, B. Zheng, H. Wang, J. Wang, S. Chen, S. Nie and M. Xie, Cultured Cordyceps sinensis polysaccharides modulate intestinal mucosal immunity and gut microbiota in cyclophosphamide-treated mice, *Carbohydr Polym*, 2020, **235**, 115957.

28.   X. Wang, C. X. Hai, X. Liang, S. X. Yu, W. Zhang and Y. L. Li, The protective

effects of Acanthopanax senticosus Harms aqueous extracts against oxidative stress: role of Nrf2 and antioxidant enzymes, *J Ethnopharmacol*, 2010, **127**, 424-432.

29. S. Tsukamoto-Sen, S. Kawakami, H. Maruki-Uchida, R. Ito, N. Matsui, Y. Komiya, Y. Mita, M. Morisasa, N. Goto-Inoue, Y. Furuichi, Y. Manabe, M. Morita and N. L. Fujii, Effect of antioxidant supplementation on skeletal muscle and metabolic profile in aging mice, *Food Funct*, 2021, **12**, 825-833.

30. F. Bianchi, M. Dall'Asta, D. D. Rio, A. Mangia, M. Musci and F. Scazzina, Development of a headspace solid-phase microextraction gas chromatography–mass spectrometric method for the determination of short-chain fatty acids from intestinal fermentation, *Food Chemistry*, 2011, **129**, 200-205.

31. A. Winkelstein, Mechanisms of immunosuppression: effects of cyclophosphamide on cellular immunity, *Blood*, 1973, **41**, 273-284.

32. A. R. Ahmed and S. M. Hombal, Cyclophosphamide (Cytoxan). A review on relevant pharmacology and clinical uses, *J Am Acad Dermatol*, 1984, **11**, 1115-1126.

33. G. B. McDonald, J. T. Slattery, M. E. Bouvier, S. Ren, A. L. Batchelder, T. F. Kalhorn, H. G. Schoch, C. Anasetti and T. Gooley, Cyclophosphamide metabolism, liver toxicity, and mortality following hematopoietic stem cell transplantation, *Blood*, 2003, **101**, 2043-2048.

34. C. Li, S. Duan, Y. Li, X. Pan and L. Han, Polysaccharides in natural products that repair the damage to intestinal mucosa caused by cyclophosphamide and their mechanisms: A review, *Carbohydr Polym*, 2021, **261**, 117876.

35. G. Cai, Y. Wu, A. Wusiman, P. Gu, N. Mao, S. Xu, T. Zhu, Z. Feng, Z. Liu and D. Wang, Alhagi honey polysaccharides attenuate intestinal injury and immune suppression in cyclophosphamide-induced mice, *Food Funct*, 2021, **12**, 6863-6877.

36. G. La Fata, P. Weber and M. H. Mohajeri, Probiotics and the Gut Immune System: Indirect Regulation, *Probiotics Antimicrob Proteins*, 2018, **10**, 11-21.

37. X. H. Wang, Z. H. Yuan, L. J. Zhu, X. L. Yi, Z. P. Ou, R. F. Li, Z. L. Tan, B. Pozniak, B. Obminska-Mrukowicz, J. Wu and J. N. Yi, Protective effects of betulinic acid on intestinal mucosal injury induced by cyclophosphamide in mice, *Pharmacol Rep*, 2019, **71**, 929-939.

38. X. Han, B. Bai, Q. Zhou, J. Niu, J. Yuan, H. Zhang, J. Jia, W. Zhao and H. Chen, Dietary supplementation with polysaccharides from Ziziphus Jujuba cv. Pozao intervenes in immune response via regulating peripheral immunity and intestinal barrier function in cyclophosphamide-induced mice, *Food Funct*, 2020, **11**, 5992-6006.

39. J. Yang, K. X. Liu, J. M. Qu and X. D. Wang, The changes induced by cyclophosphamide in intestinal barrier and microflora in mice, *Eur J Pharmacol*, 2013, **714**, 120-124.

40. R. Wei, J. Wirkus, Z. Yang, J. Machuca, Y. Esparza and G. G. Mackenzie, EGCG sensitizes chemotherapeutic-induced cytotoxicity by targeting the ERK

pathway in multiple cancer cell lines, *Archives of biochemistry and biophysics*, 2020, **692**, 108546.

41.   M. A. Potenza, F. L. Marasciulo, M. Tarquinio, E. Tiravanti, G. Colantuono, A. Federici, J. A. Kim, M. J. Quon and M. Montagnani, EGCG, a green tea polyphenol, improves endothelial function and insulin sensitivity, reduces blood pressure, and protects against myocardial I/R injury in SHR, *Am J Physiol Endocrinol Metab*, 2007, **292**, E1378-1387.

42.   M. L. Wan, K. H. Ling, M. F. Wang and H. El-Nezami, Green tea polyphenol epigallocatechin-3-gallate improves epithelial barrier function by inducing the production of antimicrobial peptide pBD-1 and pBD-2 in monolayers of porcine intestinal epithelial IPEC-J2 cells, *Mol Nutr Food Res*, 2016, **60**, 1048-1058.

43.   C. Carrasco-Pozo, P. Morales and M. Gotteland, Polyphenols protect the epithelial barrier function of Caco-2 cells exposed to indomethacin through the modulation of occludin and zonula occludens-1 expression, *J Agric Food Chem*, 2013, **61**, 5291-5297.

44.   C. Di Lorenzo, F. Colombo, S. Biella, C. Stockley and P. Restani, Polyphenols and Human Health: The Role of Bioavailability, *Nutrients*, 2021, **13**.

45.   A. Takagaki and F. Nanjo, Metabolism of (-)-epigallocatechin gallate by rat intestinal flora, *J Agric Food Chem*, 2010, **58**, 1313-1321.

46.   K. Nakagawa and T. Miyazawa, Absorption and distribution of tea catechin, (-)-epigallocatechin-3-gallate, in the rat, *J Nutr Sci Vitaminol (Tokyo)*, 1997, **43**, 679-684.

47.   J. M. Anderson, Molecular structure of tight junctions and their role in epithelial transport, *News Physiol Sci*, 2001, **16**, 126-130.

48.   F. Sanchez de Medina, I. Romero-Calvo, C. Mascaraque and O. Martinez-Augustin, Intestinal inflammation and mucosal barrier function, *Inflamm Bowel Dis*, 2014, **20**, 2394-2404.

49.   J. M. Zhang and J. An, Cytokines, inflammation, and pain, *Int Anesthesiol Clin*, 2007, **45**, 27-37.

50.   T. Bedke, F. Muscate, S. Soukou, N. Gagliani and S. Huber, IL-10-producing T cells and their dual functions, *Semin Immunol*, 2019, **44**, 101335.

51.   F. N. Lauw, D. Pajkrt, C. E. Hack, M. Kurimoto, S. J. van Deventer and T. van der Poll, Proinflammatory effects of IL-10 during human endotoxemia, *J Immunol*, 2000, **165**, 2783-2789.

52.   H. Tilg, C. van Montfrans, A. van den Ende, A. Kaser, S. J. van Deventer, S. Schreiber, M. Gregor, O. Ludwiczek, P. Rutgeerts, C. Gasche, J. C. Koningsberger, L. Abreu, I. Kuhn, M. Cohard, A. LeBeaut, P. Grint and G. Weiss, Treatment of Crohn's disease with recombinant human interleukin 10 induces the proinflammatory cytokine interferon gamma, *Gut*, 2002, **50**, 191-195.

53.   E. B. Byun, W. S. Kim, N. Y. Sung and E. H. Byun, Epigallocatechin-3-Gallate Regulates Anti-Inflammatory Action Through 67-kDa Laminin Receptor-Mediated Tollip Signaling Induction in Lipopolysaccharide-Stimulated Human Intestinal Epithelial Cells, *Cell Physiol Biochem*, 2018, **46**, 2072-2081.

54. Z. T. Bitzer, R. J. Elias, M. Vijay-Kumar and J. D. Lambert, (-)-Epigallocatechin-3-gallate decreases colonic inflammation and permeability in a mouse model of colitis, but reduces macronutrient digestion and exacerbates weight loss, *Mol Nutr Food Res*, 2016, **60**, 2267-2274.

55. G. Feng, S. Laijin, S. Chen, W. Teng, Z. Dejian, C. Yin and G. Shoudong, In vitro and in vivo immunoregulatory activity of sulfated fucan from the sea cucumber A. leucoprocta, *Int J Biol Macromol*, 2021, **187**, 931-938.

56. A. Thomson, D. Hemphill and K. N. Jeejeebhoy, Oxidative stress and antioxidants in intestinal disease, *Dig Dis*, 1998, **16**, 152-158.

57. A. Bhattacharyya, R. Chattopadhyay, S. Mitra and S. E. Crowe, Oxidative stress: an essential factor in the pathogenesis of gastrointestinal mucosal diseases, *Physiol Rev*, 2014, **94**, 329-354.

58. R. Jeelani, S. N. Khan, F. Shaeib, H. R. Kohan-Ghadr, S. R. Aldhaheri, T. Najafi, M. Thakur, R. Morris and H. M. Abu-Soud, Cyclophosphamide and acrolein induced oxidative stress leading to deterioration of metaphase II mouse oocyte quality, *Free Radic Biol Med*, 2017, **110**, 11-18.

59. M. Sulkowska, S. Sulkowski, E. Skrzydlewska and R. Farbiszewski, Cyclophosphamide-induced generation of reactive oxygen species. Comparison with morphological changes in type II alveolar epithelial cells and lung capillaries, *Exp Toxicol Pathol*, 1998, **50**, 209-220.

60. S. Shruthi and K. B. Shenoy, Gallic acid: A promising genoprotective and hepatoprotective bioactive compound against cyclophosphamide induced toxicity in mice, *Environ Toxicol*, 2020, DOI: 10.1002/tox.23018.

61. B. Sanchez, S. Delgado, A. Blanco-Miguez, A. Lourenco, M. Gueimonde and A. Margolles, Probiotics, gut microbiota, and their influence on host health and disease, *Mol Nutr Food Res*, 2017, **61**.

62. W. Jia, H. Li, L. Zhao and J. K. Nicholson, Gut microbiota: a potential new territory for drug targeting, *Nat Rev Drug Discov*, 2008, **7**, 123-129.

63. Y. Ding, Y. Yan, D. Chen, L. Ran, J. Mi, L. Lu, B. Jing, X. Li, X. Zeng and Y. Cao, Modulating effects of polysaccharides from the fruits of Lycium barbarum on the immune response and gut microbiota in cyclophosphamide-treated mice, *Food Funct*, 2019, **10**, 3671-3683.

64. F. Magne, M. Gotteland, L. Gauthier, A. Zazueta, S. Pesoa, P. Navarrete and R. Balamurugan, The Firmicutes/Bacteroidetes Ratio: A Relevant Marker of Gut Dysbiosis in Obese Patients?, *Nutrients*, 2020, **12**.

65. S. Stojanov, A. Berlec and B. Strukelj, The Influence of Probiotics on the Firmicutes/Bacteroidetes Ratio in the Treatment of Obesity and Inflammatory Bowel disease, *Microorganisms*, 2020, **8**.

66. N. A. Nagalingam, J. Y. Kao and V. B. Young, Microbial ecology of the murine gut associated with the development of dextran sodium sulfate-induced colitis, *Inflamm Bowel Dis*, 2011, **17**, 917-926.

67. X. Ma, Y. Hu, X. Li, X. Zheng, Y. Wang, J. Zhang, C. Fu and F. Geng, Periplaneta americana Ameliorates Dextran Sulfate Sodium-Induced Ulcerative Colitis in Rats by Keap1/Nrf-2 Activation, Intestinal Barrier Function,

and Gut Microbiota Regulation, *Front Pharmacol*, 2018, **9**, 944.

68.   L. E. Ritchie, J. M. Sturino, R. J. Carroll, L. W. Rooney, M. A. Azcarate-Peril and N. D. Turner, Polyphenol-rich sorghum brans alter colon microbiota and impact species diversity and species richness after multiple bouts of dextran sodium sulfate-induced colitis, *FEMS Microbiol Ecol*, 2015, **91**.

69.   M. Rau, A. Rehman, M. Dittrich, A. K. Groen, H. M. Hermanns, F. Seyfried, N. Beyersdorf, T. Dandekar, P. Rosenstiel and A. Geier, Fecal SCFAs and SCFA-producing bacteria in gut microbiome of human NAFLD as a putative link to systemic T-cell activation and advanced disease, *United European Gastroenterol J*, 2018, **6**, 1496-1507.

70.   M. Remely, F. Ferk, S. Sterneder, T. Setayesh, S. Roth, T. Kepcija, R. Noorizadeh, I. Rebhan, M. Greunz, J. Beckmann, K. H. Wagner, S. Knasmuller and A. G. Haslberger, EGCG Prevents High Fat Diet-Induced Changes in Gut Microbiota, Decreases of DNA Strand Breaks, and Changes in Expression and DNA Methylation of Dnmt1 and MLH1 in C57BL/6J Male Mice, *Oxid Med Cell Longev*, 2017, **2017**, 3079148.

71.   D. Rios-Covian, P. Ruas-Madiedo, A. Margolles, M. Gueimonde, C. G. de Los Reyes-Gavilan and N. Salazar, Intestinal Short Chain Fatty Acids and their Link with Diet and Human Health, *Front Microbiol*, 2016, **7**, 185.

72.   T. Okubo, N. Ishihara, A. Oura, M. Serit, M. Kim, T. Yamamoto and T. Mitsuoka, In Vivo Effects of Tea Polyphenol Intake on Human Intestinal Microflora and Metabolism, *Biosci Biotechnol Biochem*, 1992, **56**, 588-591.

73.   S. M. Henning, J. Yang, M. Hsu, R. P. Lee, E. M. Grojean, A. Ly, C. H. Tseng, D. Heber and Z. Li, Decaffeinated green and black tea polyphenols decrease weight gain and alter microbiome populations and function in diet-induced obese mice, *Eur J Nutr*, 2018, **57**, 2759-2769.

74.   M. Vacca, G. Celano, F. M. Calabrese, P. Portincasa, M. Gobbetti and M. De Angelis, The Controversial Role of Human Gut Lachnospiraceae, *Microorganisms*, 2020, **8**.

75.   J. T. Matthieu Million, Camille Wagner, Hugues Lelouard, Didier Raoult, Jean-Pierre Gorvel, New insights in gut microbiota and mucosal immunity of the small intestine, *Human Microbiome Journal*, 2018, **7-8**, 23-32.

76.   H. S. Zhang, X. F. Liao, J. B. Sparks and X. M. Luo, Dynamics of Gut Microbiota in Autoimmune Lupus, *Appl Environ Microb*, 2014, **80**, 7551-7560.

77.   P. Ojeda, A. Bobe, K. Dolan, V. Leone and K. Martinez, Nutritional modulation of gut microbiota - the impact on metabolic disease pathophysiology, *J Nutr Biochem*, 2016, **28**, 191-200.

78.   A. Everard, V. Lazarevic, M. Derrien, M. Girard, G. G. Muccioli, A. M. Neyrinck, S. Possemiers, A. Van Holle, P. Francois, W. M. de Vos, N. M. Delzenne, J. Schrenzel and P. D. Cani, Responses of gut microbiota and glucose and lipid metabolism to prebiotics in genetic obese and diet-induced leptin-resistant mice, *Diabetes*, 2011, **60**, 2775-2786.

79.   I. Lagkouvardos, T. R. Lesker, T. C. A. Hitch, E. J. C. Galvez, N. Smit, K. Neuhaus, J. Wang, J. F. Baines, B. Abt, B. Stecher, J. Overmann, T. Strowig

and T. Clavel, Sequence and cultivation study of Muribaculaceae reveals novel species, host preference, and functional potential of this yet undescribed family, *Microbiome*, 2019, **7**, 28.

80.   T. C. Shen, C. Chehoud, J. Ni, E. Hsu, Y. Y. Chen, A. Bailey, A. Laughlin, K. Bittinger, F. D. Bushman and G. D. Wu, Dietary Regulation of the Gut Microbiota Engineered by a Minimal Defined Bacterial Consortium, *PLoS One*, 2016, **11**, e0155620.

81.   M. I. Queipo-Ortuno, M. Boto-Ordonez, M. Murri, J. M. Gomez-Zumaquero, M. Clemente-Postigo, R. Estruch, F. Cardona Diaz, C. Andres-Lacueva and F. J. Tinahones, Influence of red wine polyphenols and ethanol on the gut microbiota ecology and biochemical biomarkers, *Am J Clin Nutr*, 2012, **95**, 1323-1334.

82.   M. V. Selma, D. Beltran, M. C. Luna, M. Romo-Vaquero, R. Garcia-Villalba, A. Mira, J. C. Espin and F. A. Tomas-Barberan, Isolation of Human Intestinal Bacteria Capable of Producing the Bioactive Metabolite Isourolithin A from Ellagic Acid, *Front Microbiol*, 2017, **8**, 1521.

83.   T. Clavel, C. Charrier, A. Braune, M. Wenning, M. Blaut and D. Haller, Isolation of bacteria from the ileal mucosa of TNFdeltaARE mice and description of Enterorhabdus mucosicola gen. nov., sp. nov, *Int J Syst Evol Microbiol*, 2009, **59**, 1805-1812.

84.   L. M. Bode, D. Bunzel, M. Huch, G. S. Cho, D. Ruhland, M. Bunzel, A. Bub, C. M. Franz and S. E. Kulling, In vivo and in vitro metabolism of trans-resveratrol by human gut microbiota, *Am J Clin Nutr*, 2013, **97**, 295-309.

85.   M. Kutschera, W. Engst, M. Blaut and A. Braune, Isolation of catechin-converting human intestinal bacteria, *J Appl Microbiol*, 2011, **111**, 165-175.

Table 1. Primer sequences for qRT-PCR analysis.

Gene name	Forward (5'-3')	Reverse (5'-3')
IL-10	TACCTGGTAGAAGTGATGCC	CATCATGTATGCTTCTATGC
IL-21	ATGCCCTTCCTGTGATTCGT	CCCGGACACAACATGGAAGT
TNFα	CCTCTCTCTAATCAGCCCTCTG	GAGGACCTGGGAGTAGATGAG
CAT	CAGCTCCGCAATCCTACACC	CAGCGTTGATTACAGGTGATCC
SOD1	CAGGACCTCATTTTAATCCTCAC	TGCCCAGGTCTCCAACAT
GSH-PX1	GGGACTACACCGAGATGAAC	TCCGCAGGAAGGTAAAGA
β-actin	ATGCTCTCCCTCACGCCATC	GAGGAAGAGGATGCGGCAGT

Figure legends

Figure 1. Effects of EGCG on body weight and intestinal morphology in the cyclophosphamide (CTX)-treated mice. (A) Scheme of the animal experimental design. Mice were initially treated with CTX or vehicle once daily for 5 days. On the 6th day, the non-treated mice were separated randomly into the vehicle-control group (Ctrl)

or high dose (40 mg/kg/d) EGCG group [E(H)]. Moreover, CTX-treated mice were further randomized into 3 groups, and orally gavaged daily with water (CTX group), low dose (20 mg/kg/d) EGCG [CTX+E(L)], or a high dose (40 mg/kg/d) EGCG [CTX+E(L)] for additional 25 days. **(B)** Body weight progression. Values are presented as Mean±SD. *p<0.05, **p<0.01 vs. control.* **(C)** Effects of EGCG (E) on the intestinal morphology following cyclophosphamide (CTX) treatment. Pictures were taken at x20 and x100 magnification and representative images are shown. Villi height, crypt depth and ratio of villi/crypt were measured and analyzed using the Image J software. Results are shown as Mean±SD. *p<0.05, **p<0.01 vs. control.*

Figure 2. EGCG ameliorates intestine barrier damage induced by cyclophosphamide (CTX). (A) Intestinal permeability was evaluated by measuring fluorescein isothiocyanate-dextran (FITC-Dextran) at the endpoint. Ctrl represents control while CTX, E and CTXE serve as cyclophosphamide, EGCG (40mg/kg/d), and cyclophosphamide plus EGCG (40mg/kg/d), respectively. Values are presented as fold over control. *p<0.05, **p<0.01 vs. control.* **(B)** Effects of cyclophosphamide (CTX) and EGCG (E) on the expression of the tight junction proteins. Immunoblots for ZO-1, Occludin, and Claudin-1 are shown. Loading control: GAPDH. Bands were quantified and results are presented as percentage of control. *p<0.05, **p<0.01 vs. control.*

Figure 3. EGCG mitigates IL-10, IL-21 and TNFα levels induced by cyclophosphamide (CTX). Concentrations and relative mRNA expression levels of IL-10, IL-21 and TNFα in the intestine were determined by ELISA (left) and qPCR (right) as described in the Methods section. Values are presented as Mean±SD. *p<0.05, **p<0.01 vs. control.*

Figure 4. Effects of EGCG treatment on cyclophosphamide (CTX) induced immune-suppression. At the end of the experimental period, the spleen and thymus in each group were weight, analyzed and the indices presented as percentage of body weight. *p<0.05, **p<0.01 vs. control.*

Figure 5. EGCG reduces the increase in reactive oxygen species induced by cyclophosphamide (CTX). (A) Total antioxidant capacity (T-AOC), malondialdehyde (MDA) content of the intestine tissue were measured. Values are presented as Mean±SD. *p<0.05, **p<0.01 vs. control.* **(B)** Enzymatic activities and mRNA expression levels of catalase (CAT), superoxide dismutase (SOD) and glutathione peroxidase (GSH-PX) of each group. Values are presented as Mean±SD. *p<0.05, **p<0.01 vs. control.*

Figure 6. Cyclophosphamide (CTX) affects the gut microbiota α-diversity. Shannon, Simpson and Ace, Chao 1 indexes were determined in Control (Ctrl), CTX, E and CTXE groups to evaluate the gut microbiota community diversity and richness among groups. *p<0.05 vs. control.*

Figure 7. EGCG administration regulates the microbial community distribution in cyclophosphamide (CTX)-treated mice. (A) Venn diagram analysis highlighting the spatial diversity of the bacterial genus among groups. **(B)** Stack column plot of relative taxa abundance by phylum in each group. **(C)** Ratio between Firmicutes and Bacteroidetes. *p<0.05, **p<0.01 vs. control.* **(D)** Stack column plot of relative community abundance at the family level in each group.

Figure 8. EGCG partially restores community phylotype changes induced by cyclophosphamide (CTX). (A) Principal component analysis (PCA). PC1 and PC2 represent the two most principal factors characterizing the bacterial profile and their contribution rates (%) are shown on the axes. **(B)** Partial least squares discriminant analysis (PLS-DA). COMP1 and the COMP2 are the two predicted dominating components for the variance of microbial community composition. **(C)** Distribution histogram of the LDA score determined by effect size (LEfSe). Bacterial taxa specifically enriched in groups with an LDA score > 2 are shown in the histogram.

Figure 9. Effect of EGCG on the fecal SCFAs levels of the mice treated with cyclophosphamide (CTX). Levels of acetic, propionic, isobutyric, butyric, isovaleric, valeric acids and total SCFAs of each group. Values are presented as Mean±SD. *p<0.05, **p<0.01 vs. control.*

Figure 1
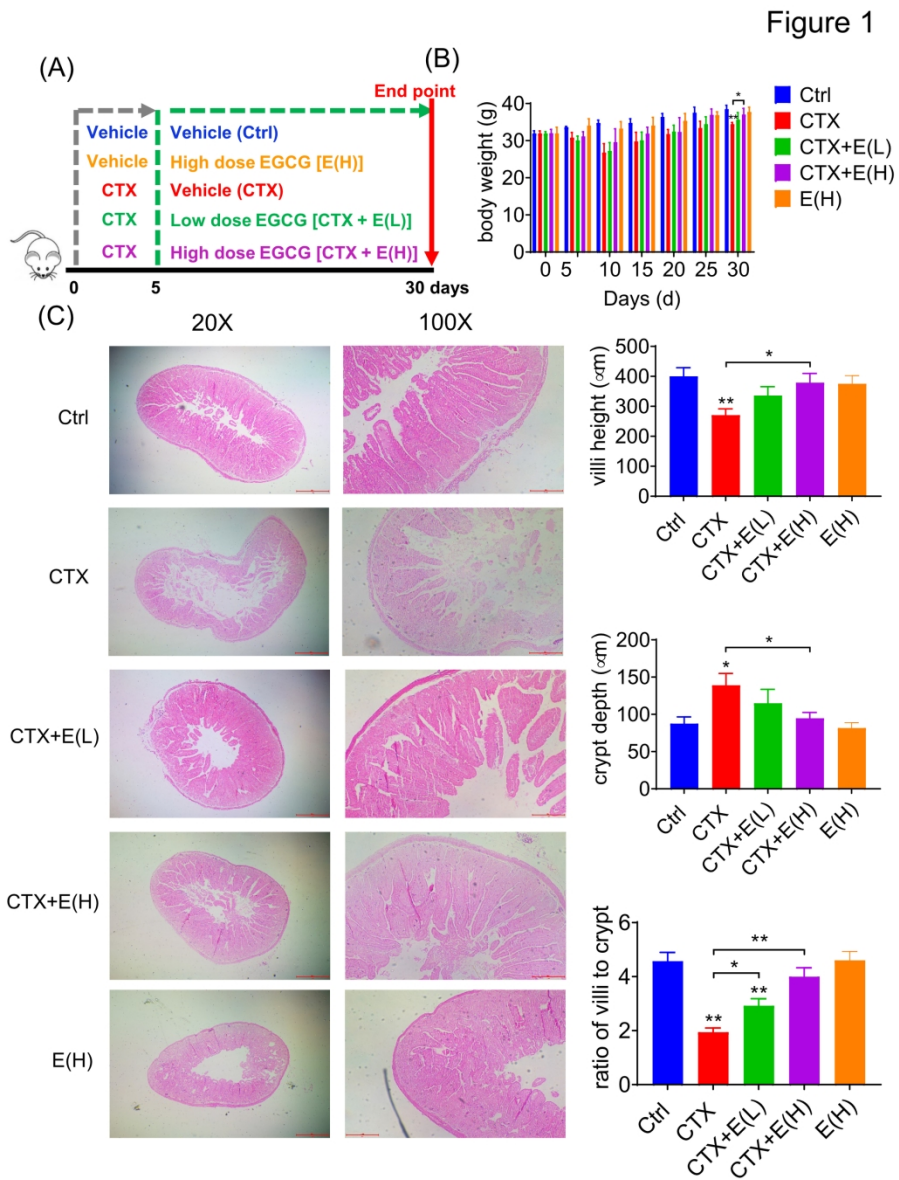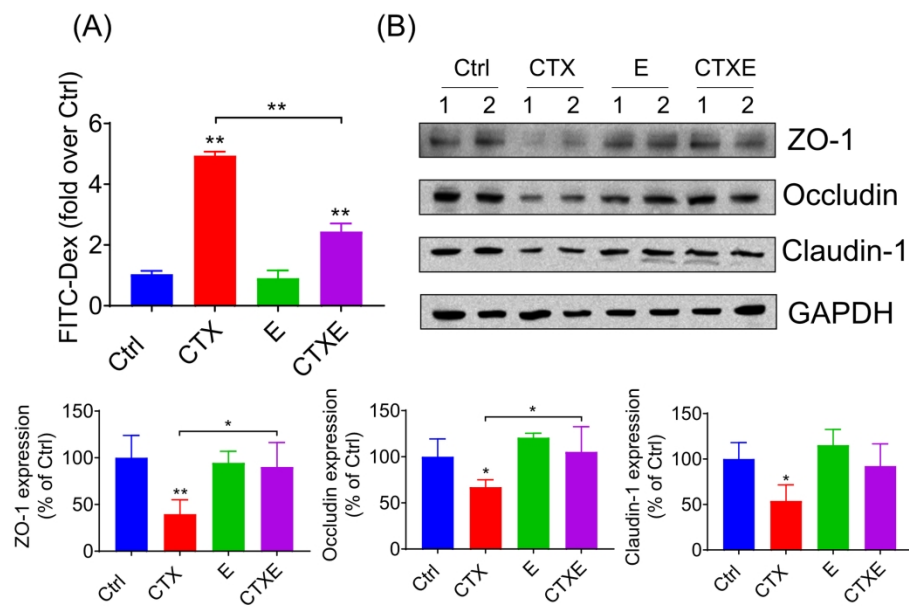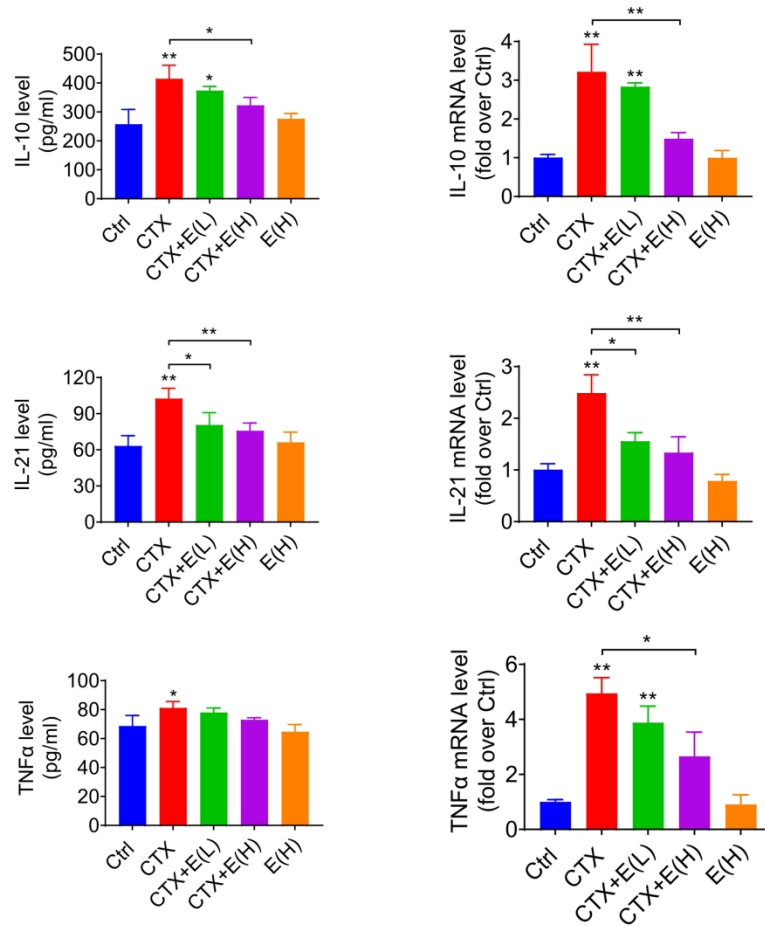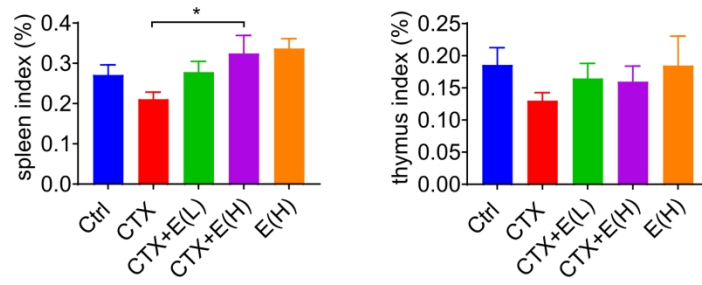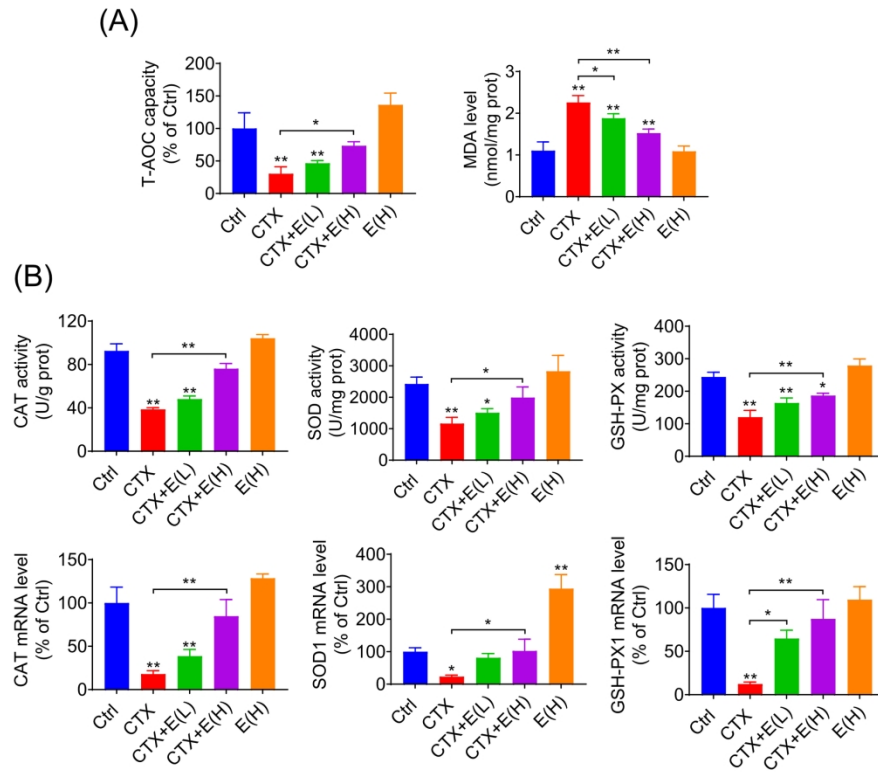
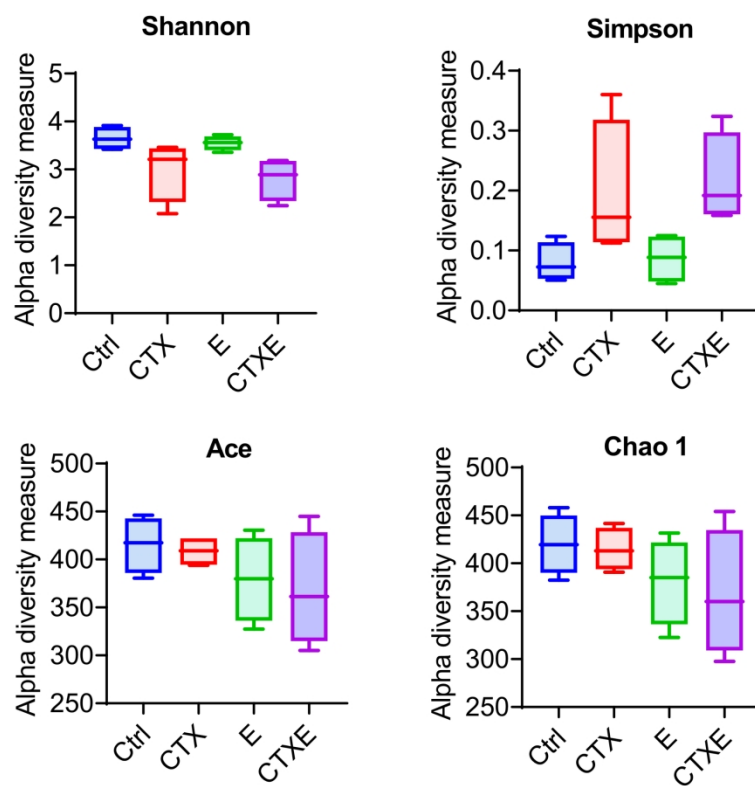190x254mm (300 x 300 DPI)
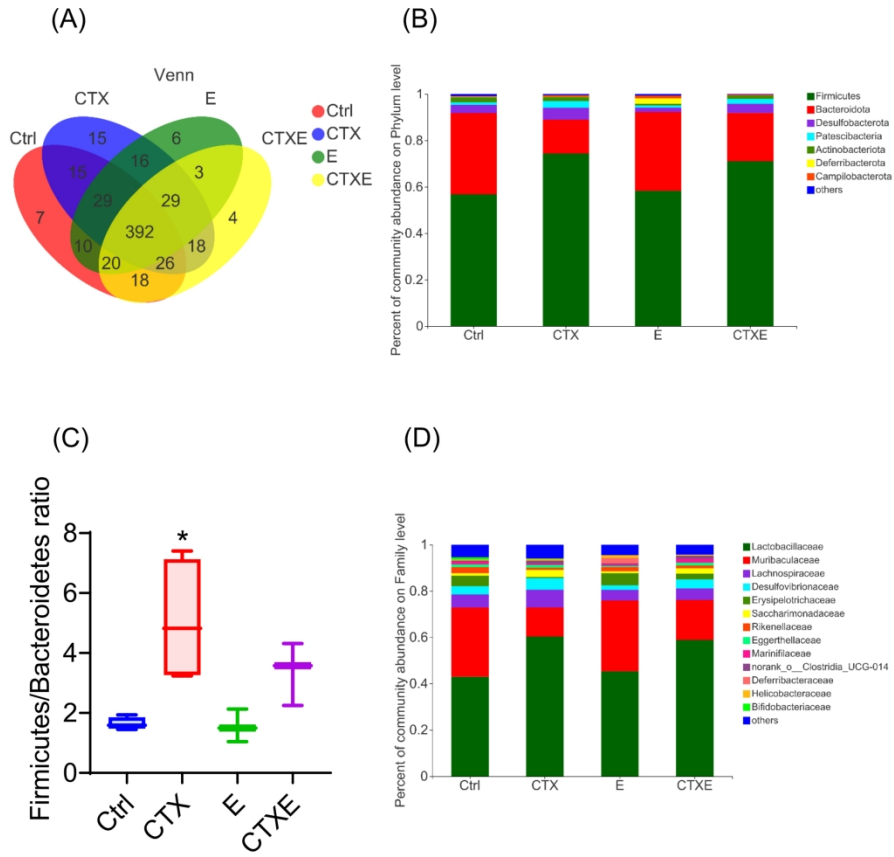
Figure 2

(A)

(B)

Figure 2

190x254mm (300 x 300 DPI)

Figure 3

Figure 3

190x254mm (300 x 300 DPI)

Figure 4

Figure 4

190x254mm (300 x 300 DPI)

Figure 5

(A)

(B)

Figure 5

190x254mm (300 x 300 DPI)

Figure 6

Figure 6

190x254mm (300 x 300 DPI)

Figure 7

(A)

(B)

(C)

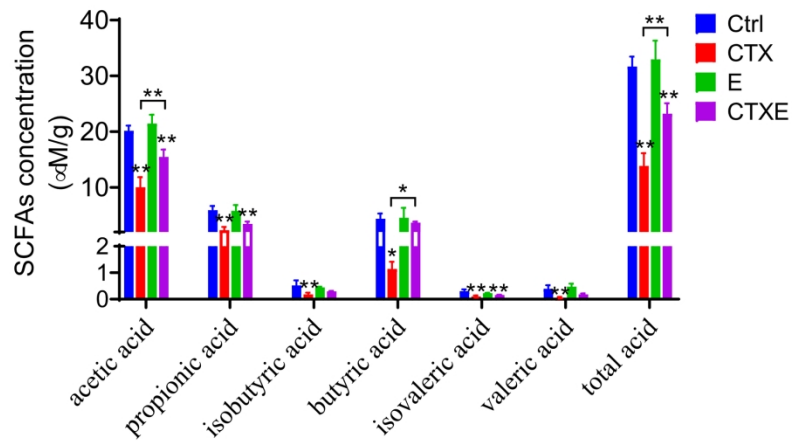(D)

Figure 7

190x254mm (300 x 300 DPI)

Figure 8

Figure 8

190x254mm (300 x 300 DPI)

Figure 9

Figure 9

190x254mm (300 x 300 DPI)